Journal of Power Sources 250 (2014) 296–305

Contents lists available at ScienceDirect

Journal of Power Sources

journal homepage: www.elsevier.com/locate/jpowsour

Study on the stability of the $LiFePO_4$ Li-ion battery via an electrochemical method

Kuan Zhong [a,b], Yan Cui [b], Xin-De Xia [b], Jian-Jun Xue [b,*], Peng Liu [a,*], Ye-Xiang Tong [a,*]

[a] School of Chemistry and Chemical Engineering, Sun Yat-Sen University, Guangzhou 510275, PR China
[b] Research and Development Department, Guangzhou Great Power Energy & Technology Co., Ltd., Guangzhou 511483, PR China

HIGHLIGHTS

- Activation affects the lithium iron phosphate battery (LIPB) stability greatly.
- Charge/discharge cycle and aging are the two key factors for LIPB stability.
- Activation affects the stability of solid-electrolyte-interface (SEI) films greatly.
- The stable SEI films are compact and mainly composed of the more "inorganic" species.
- The stable LIPB shows high open circuit voltage, capacity, and cycleability.

ARTICLE INFO

Article history:
Received 18 July 2013
Received in revised form
7 November 2013
Accepted 12 November 2013
Available online 21 November 2013

Keywords:
Lithium iron phosphate
Aging
Self-discharge
Solid-electrolyte-interface films
Activation

ABSTRACT

Lithium iron phosphate battery (LIPB) is a promising power source for electric vehicle. However, LIPBs generally show a low uniformity in performances due to their poor stability. Herein, we employ an electrochemical method to study the stability of LIPB, and the results show that stable LIPB can be obtained by using the activation with both charge–discharge cycle and aging, since the stable solid-electrolyte-interface (SEI) films are available. The stable SEI films are associated with the low self-discharge of LIPB, characterized by keeping high open circuit voltage (OCV) during storage under discharged states, high capacity, stable internal resistance, and high charge/discharge reversibility. Most of the low-OCV LIPBs can be repaired by using the electrochemical treatment containing charge–discharge cycle and aging. The activation processes with charge–discharge cycle and aging induce the generation of the smooth, adherent, and stable SEI films, contributing to the good stability of the battery. The achievement of the stable SEI films is mainly resulted from the formation of the surface layers completely covering the electrodes' surfaces during charge–discharge cycle, and the stabilization of the layers by transforming the layers' species to the "more inorganic" compounds such as carboxylates or even carbonates (like Li_2CO_3) during aging.

1. Introduction

The stability of a Li-ion battery plays an important role in its practical application, especially for the electric vehicle-used batteries. The stability of a battery is generally affected by the properties of electrode materials, the composition of electrolyte, and the post-treatments [here mainly means activation processes (also called as formation in industry)] to a new battery. The effects of electrolyte, supporting electrolyte, and electrolyte additives on the properties of a Li-ion battery and the interactions between electrolyte and electrodes both have been studied extensively [1–6]. In addition, the relationship between the stability of electrode materials and their compositions, morphologies, particle sizes, structures, and surface states were also addressed [7–9]. Li-ion battery has been obtained great development thanks to the optimizations of the properties of electrode materials and electrolyte. However, less effort contributes to the systematic investigation of the effects of activation processes on the stability of the lithium iron phosphate battery (LIPB) (the Li-ion battery with $LiFePO_4$ as the cathode active material). We will present in this paper that LIPB still cannot reach stable states if the activation processes are improper even though the used battery materials are sophisticated and the battery assembly technology is advanced. Concerning the solid-electrolyte-

* Corresponding authors. Tel.: +86 20 84110071; fax: +86 20 84112245, +86 20 39196767.
E-mail addresses: zhongk@mail.sysu.edu.cn, zhongk2w@yahoo.cn (K. Zhong), ycui_gp@163.com (Y. Cui), xdxia_gp@163.com (X.-D. Xia), xueorjj@163.com (J.-J. Xue), ceslp@mail.sysu.edu.cn (P. Liu), chedhx@mail.sysu.edu.cn (Y.-X. Tong).

0378-7753/$ – see front matter © 2013 Elsevier B.V. All rights reserved.
http://dx.doi.org/10.1016/j.jpowsour.2013.11.019

interface (SEI) films, the stability of a battery is generally studied only in the first charge process from the respect of activation processes. However, the "good stability" of the SEI films formed in the first charge process is likely temporary (e.g., occurrence of capacity fading upon storage), which is still detrimental to the battery practical application, especially for a battery pack. In this paper, we for the first time systematically investigate the stability of LIPB in terms of activation processes.

$LiFePO_4$ material shows promising applications in electric vehicle and hybrid electric vehicle batteries due to its not too high operation voltage, high thermal stability, high charge/discharge reversibility, good cycleability, abundant resources, and non-toxicity. Studying the stability of LIPB means a great significance since the stability is directly related to the lifetime and normal operation of an LIPB pack.

The effects of porosity, particle sizes, crystallinity, surface states, doping, and carbon coating on the electrochemical properties of $LiFePO_4$ have been investigated extensively [7,8,10]. The major drawback of $LiFePO_4$ is its poor conductivity, which has been overcome through adding conductive carbon [11–13], optimizing morphology [14,15], doping functional materials, and incorporating nanostructured designs [9,16,17]. However, LIPB still cannot achieve stable states (such as occurrence of large self-discharge) if the activation processes are improper since the processes can affect greatly the stability of the LIPB by affecting the stability of SEI films, as will be discussed in this paper.

Low open circuit voltage (OCV) issue generally occurs on LIPB, which can damage the uniformity in the electrochemical performances of an LIPB pack, causing a decrease in the cycle life of the battery pack. The low voltage issue is mainly derived from the self-discharge of a battery, which can arise from a side reaction (caused by foreign matters) [18], inner short circuiting, and the unstability of the formed SEI films (unstable adsorbate-induced self-discharge) [8,19]. The former two problems can be resolved by using the high purified materials and optimizing the technology designs. Only the low voltage issue derived from the unstable SEI films can be tackled with proper charge/discharge parameters and other repaired treatments, which was obtained less attention.

In addition, the formed SEI films have been found to be a key component affecting important cell performances, such as cycle life, irreversible capacity loss, safety, and others [20–23]. For example, the dissolution of SEI films during cycling or storage (especially at high temperatures) has been claimed to be a major cause for capacity fading [24–26], since film dissolution can result in the exposure of the electrode surface to electrolyte, prompting irreversible reactions between the electrode and the electrolyte. This kind of self-discharge is generally unrecoverable. Therefore, to obtain the stable SEI films is of great significance.

Much attention was thrown on the achievement of stable SEI films by adding additives in electrolyte and optimizing the morphologies, structures, and surfaces states of active materials [1]. However, the capacity loss during storage at different temperatures and the poor cycling properties still can occur if the improper activation processes are applied, which is generally neglected.

It is well-known that decreasing $LiFePO_4$ particle sizes to nanometer scale can increase the particles' conductivity. On the other hand, decreasing the particle sizes also can lead to an increase in the electrode's surface area and thus to a subsequent amplification of the parasitic reactions occurring on the electrode–electrolyte interfaces. This is responsible for the occurrence of the large self-discharge in a battery. Besides, the nanostructures exhibit higher surface energy which can induce numerous adsorbates and thus cause self-discharge if such adsorbed species are unstable. Therefore, to make the formed SEI films stable to avoid the catalyzed reactions that deteriorate the properties of the active materials [27,28] or the formation of the unstable resistive layer from the electrolyte decomposition products [29–31] is greatly meaningful.

In addition, $LiFePO_4$ particles show surface reactivity upon immersion in the classical $LiPF_6$ electrolyte [4], but a carbon coating can inhibit the formation of surface species and also can hinder iron dissolution at elevated temperatures. Otherwise, iron can be dissolved by the acidic species in the electrolyte at a temperature higher than 40 °C [32]. Thus, it is important to make the SEI films cover completely the active materials prior to exposure of the battery to a high temperature environment. This can be achieved by using the proper activation processes. Of course, the physicochemical properties of the active materials must be taken into account.

The surfaces of carbon-coated $LiFePO_4$ particles can form surface lithium species under storage at elevated temperatures (>40 °C), and the formed surface films gradually turn to stable with duration [8] when an LIPB has a certain state of charge (SOC). For the LIPB using the $LiFePO_4$ particles with incomplete, less or no carbon coating, the surfaces of the particles soaked in electrolyte can form abundant lithium species which are difficult to reach a stable state [8]. The unstable SEI films formed by appreciable surface lithium species can be reflected by OCV [8,19]. What's more, such unstable SEI films can facilely cause self-discharge, directly leading to a decrease in OCV. Understanding these phenomena allow us to choose the proper electrode materials and to set the proper activation parameters to treat a new assembled LIPB as well as repair a low OCV battery.

A change in internal resistance also can reflect the stability of a battery. When a battery is assembled completely, the variety in internal resistance is mainly dependent on the evolution of the surface passivation films formed on both anode and cathode. The unstable surface films lead to the unstable internal resistance.

In this study, we investigate the stability of LIPB by using different activation processes because they can affect the stability of the formed SEI films. The stability of SEI films is closely related to the self-discharge of an LIPB. The self-discharge can be characterized by the OCV evolution of the battery, especially when the battery is stored at high temperatures in discharged states (we call this process as a self-discharge experiment in this study) because a relatively small self-discharge can lead to a relatively large OCV change. In addition, we also concern the capacity property and internal resistance variety of LIPB since they are also related to the stability of SEI films. For further elucidating the relationship between activation processes and the stability of SEI films, we try to repair the low-OCV LIPB by employing the proper charge/discharge steps and other treatments. The formation of SEI films is also proved by scanning electron microscopy (SEM), energy dispersive X-ray spectroscopy (EDS), and Fourier transformation infrared spectroscopy (FTIR).

2. Experimental

Both $LiFePO_4$ and graphite used were commercial products. The positive active material of $LiFePO_4$ particles with Mg^{2+} doping (for improving conductivity and cycleability [33]) and carbon coating was purchased from NanoChem Systems (Suzhou) Co., Ltd. with the product type of NCS® (the specific capacity is 135 mAh g^{-1} and the particle sizes are less than 200 nm). Graphite with F-doping (for increasing capacity and charge–discharge efficiency [34]) and surface mild oxidation treatment was obtained from Shanghai Shanshan Tech Co., Ltd. with the product type of CAG-3 (the specific capacity was ca. 320 mAh g^{-1}). We assembled dozens of 18650-type batteries to investigate the effects of activation processes on the stability and uniformity of the batteries.

The positive electrode materials were prepared by making a slurry of 96 wt % $LiFePO_4$, 1 wt % conducting carbon black, and 3 wt % polyvinylidene fluoride (PVDF) binder in *N*-methyl-2-pyrrolidone (NMP). The negative electrode materials were prepared with 91.5 wt % graphite, 1.5 wt % carbon black, 1.5 wt % conducting graphite (KS-6, NCM), 5 wt % PVDF binder and NMP solvent. Aluminum (0.020 mm in thickness) and copper foils (0.009 mm in thickness) were used as cathode and anode current collectors, respectively. The surface densities (double sides excluding the current collectors) were 25.0 ± 0.3 mg cm^{-2} for positive electrode and 11.2 ± 0.3 mg cm^{-2} for negative electrode.

The positive and negative electrodes and a Celgard 2321 triple-layer polypropylene-based membrane separator were winded into a battery core for an 18650-type battery. The used electrolyte was $LiPF_6$ (1 mol L^{-1}) – ethylene carbonate (40 wt %) – dimethyl carbonate (40 wt %) – propylene carbonate (18 wt %) – vinylene carbonate (2 wt %).

The normal capacity of an 18650-type LIPB was designed to be 1100 mAh (so the charge/discharge rate of 1 C is equivalent to 1100 mA). Prior to activation, the new LIPBs were stored at room temperature for 12 h and further at 45 °C for another 12 h in order to wet the active materials fully by electrolyte. The charge/discharge experiments were preformed at different C rates between 2.00 and 3.65 V at room temperature by using a battery testing system (CT-3008W-5V3A-S1, Neware Technology Limited).

Aging here means storage of the LIPB with a full charged state at a high temperature for a certain period (such as 2 or 4 days). Too high aging temperature (such as 60 °C) may dissolve the formed SEI films and enhance the side reactions in electrode–electrolyte interfaces, not beneficial for the stability of the SEI films. A lower aging temperature (such as room temperature) cannot effectively convert the SEI films to the stable states. Therefore, a moderate high aging temperature of 45 °C was used in this paper.

The self-discharge experiment here means storage of the LIPB with a discharged state at a high temperature for a certain period. The goal is to study the stability of the SEI films which affect self-discharge of the LIPB. The self-discharge degree can be reflected by OCV and its variety during battery storage. The self-discharge experiment was carried out as follows: the full charged LIPB was discharged at 1.00 C to 2.00 V with the discharge time limited to 90 min; after laid up for 10 min, the battery was further discharged at 0.20 C to 2.00 V with the discharge time limited to 20 min. Then, the OCV of the battery was recorded during storage at 45 °C for 4 days. A battery was considered to be stable if its OCV was higher than 2.50 V and the OCV variety was smaller than 0.10 V after 4-day storage. That is to say, the formed SEI films are stable for the battery with the above characteristics. The internal resistance (determined based on a fourpoint probe method with the AC impedance at 1 kHz) and OCV measurements were carried out with an internal-resistance-of-battery meter (BK-300, Guangzhou Blue-Key Electronic Industry Co., Ltd.).

For comparison, all of the capacities of LIPBs were measured as follow: the full charged LIPBs were discharged to 2.00 V at 1.00 C with the discharge time limited to 90 min. The battery capacity was considered to be eligible if the discharge time longer than 60 min (i.e. the capacity larger than the normal capacity 1100 mAh); otherwise the battery was considered as a low-capacity one.

The morphologies and compositions of the electrodes' surfaces were characterized by using a thermal field emission environmental scanning electron microscope (FEI/OXFORD/HKL Quanta 400F) equipped with an energy dispersive X-ray spectrometer. The surface states of the electrodes were analyzed by employing Fourier transformation IR (EQUINOX 55) with an IR microscope (Bruker). IR spectra were recorded with the diffuse reflectance mode at room temperature. The samples were all cleaned by ethyl acetate prior to surface analyses.

3. Results and discussion

Fig. 1 shows the OCV evolution of LIPB after discharged to 2.00 V. The increase in OCV indicates the Li^+ ion diffusion control in a $LiFePO_4$ material due to its intrinsic low conductivity (this process is also denoted as "relaxation"). The increase in OCV also implies the LIPB after discharged to 2.00 V still have some SOC. On the other hand, the formed surface films on the electrodes also can affect OCV as mentioned in the Introduction. Self-discharge will occur if the formed SEI films are unstable, leading to a decrease in OCV. Therefore, the evolution of OCV is the comprehensive result of relaxation and the unstable SEI film-induced self-discharge. The former affects the OCV evolution after finishing charge/discharge steps (the affecting time is only about 60 min as shown in Fig. 1), and the latter influences the OCV evolution during a long time (such as several days or even several months) storage. It is expected that the higher the OCV, the lower the self-discharge, and the better the stability of the LIPB, with the prerequisites of the same battery materials used and the same battery assembly technology adopted (i.e. the impedance of Li^+ diffusion in electrolyte, charge transfer impedance, and the package resistance of 18650 are basically the same for each battery).

The main goals of activation processes are to activate the battery materials and to induce the formation of the stable SEI films on both the negative and the positive electrodes. Various activation parameters (mainly 4 sets of activation parameters as shown in Table 1) are studied in this work in order to obtain a stable LIPB except for activating the active materials. It is generally accepted that a low-current charge can form the more stable SEI films mainly composed of organic lithium salts in addition to hindering gas generation in the first charge. So, we first use the activation processes with a low-current charge but without charge–discharge cycle or aging to treat the new LIPBs, as indicated in Table 1. The corresponding batteries are denoted as LIPB I.

Self-discharge can cause capacity loss during battery storage. The capacity loss generally induces OCV decrease, especially for the discharged battery. Storage of a battery at a relatively high temperature generally enhances self-discharge. So we study the self-discharge issue of the LIPBs with discharged states by measuring the OCV varieties during storage of the batteries at a moderate high temperature. These processes are also called as the self-discharge test (see the "Experimental" section for detail). We will also present that the low-OCV LIPB causes more capacity loss, which is also resulted from self-discharge.

Fig. 2a shows the OCV evolution of LIPB I in self-discharge test. The OCV distributions are disperse before battery storage and the

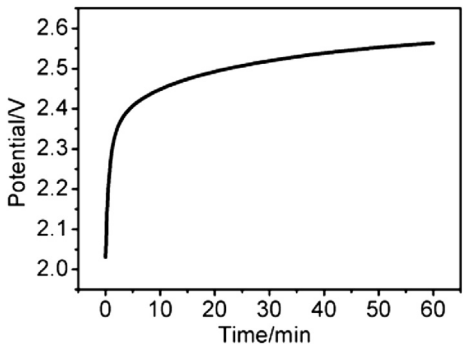

Fig. 1. Evolution of OCV with time for an LIPB after discharged to 2.00 V.

Table 1
Activation parameters for different classes of LIPB.

Activation parameters	Classes of LIPB			
	I	II	III	IV
(1) Constant current/voltage controlled charge at 0.20 C to 3.65 V with the cut-off current of 0.05 C and the charge time limited to 420 min, followed by 10-min relaxation;	▲	▲	▲	▲
(2) Constant current discharge at 0.50 C to 2.00 V with the discharge time limited to 180 min, followed by 10-min relaxation;	▲	▲	▲	▲
(3) Constant current/voltage controlled charge at 0.50 C to 3.65 V with the cut-off current of 0.05 C and the charge time limited to 180 min, followed by 10-min relaxation.	▲	▲	▲	▲
(4) Constant current discharge at 1.00 C to 2.00 V with the discharge time limited to 90 min, followed by 10-min relaxation;		▲	▲	▲
(5) Cycling the above two steps, (3) and (4), for one time.		▲	▲	
(6) Constant current/voltage controlled charge at 0.50 C to 3.65 V with the cut-off current of 0.05 C and the charge time limited to 180 min;			▲	▲
(7) Aging the full charged batteries at 45 °C for 4 days.			▲	▲

Note: The mark "▲" denotes one class of LIPB is treated by the corresponding activation parameters.

OCVs are low especially after 4-day storage of the batteries. The average OCVs (OCVs lower than 2.00 ± 0.10 V are not counted into the average values due to their distributions far from the main body) of LIPB I before and after storage are calculated to be 2.49 and 2.21 V, respectively. Herein, we employ 2.50 V, almost equal to the average OCV of LIPB I (2.49 V) before storage, to differentiate the low- or the normal-OCV LIPB. The low OCV of LIPB I (as compared to other case discussed below, 2.49 V is a much lower value) after self-discharge test suggests that a large self-discharge occurs. In addition, the batteries with OCV variety larger than 0.10 V in self-discharge test take up 61.5%, implying the great unstability of such batteries. Therefore, the LIPBs treated by the simple activation processes cannot reach stable states.

Next we add a step of charge–discharge cycle in the activation processes (as indicated in Table 1) prior to self-discharge test to study the effect of charge–discharge cycle on the stability of the battery. The batteries treated by such processes are denoted as LIPB II.

We can obtain from Fig. 2b that the average OCVs of LIPB II before and after one- and 4-day storage at 45 °C are 2.70, 2.67, and 2.60 V, respectively (the OCVs lower than 2.50 V are not included in the average values, the same below), larger than those of LIPB I. This means that charge–discharge cycle is conductive to the stability of the battery mainly derived from the more stable SEI films available in the presence of the charge–discharge cycle [14].

However, the OCV distribution of LIPB II is also disperse after self-discharge test as shown in Fig. 2b, reflecting the low uniformity in the performances of the resulting batteries. In addition, the OCVs decrease after one-day storage and further decrease after 4-day storage (Fig. 2b), indicating the large self-discharge and so the poor stability LIPB II presented.

The low-OCV LIPB II after self-discharge test takes up 26.7%, which indicates that only charge–discharge cycle cannot yield stable SEI films. On the other hand, a battery cannot achieve a stable state if its OCV variety is large even though its OCV is still rather high after self-discharge test. The LIPB II with OCV variety larger than 0.10 V takes up as large as 55.6%, indicating the quite low stability of the batteries. It is reported that the unstable SEI films could be dissolved and destructed during storage of a battery especially at high temperatures [24–26], leading to a decrease in OCV in addition to a loss in capacity. Nevertheless, we can get a hint that consolidating the stability of the SEI films formed during charge–discharge cycle prior to self-discharge test can increase OCV.

In the following, we use the activation processes involving charge–discharge cycle and aging (as shown in Table 1) to treat the new LIPBs. The obtained batteries are denoted as LIPB III. The results of self-discharge test (Fig. 2c) show that the OCV distributions are highly uniform and most OCVs are higher than 2.80 V. In addition, almost every battery's OCV increases after one-day storage, just opposite to the case in LIPB II, which indicates LIPB III

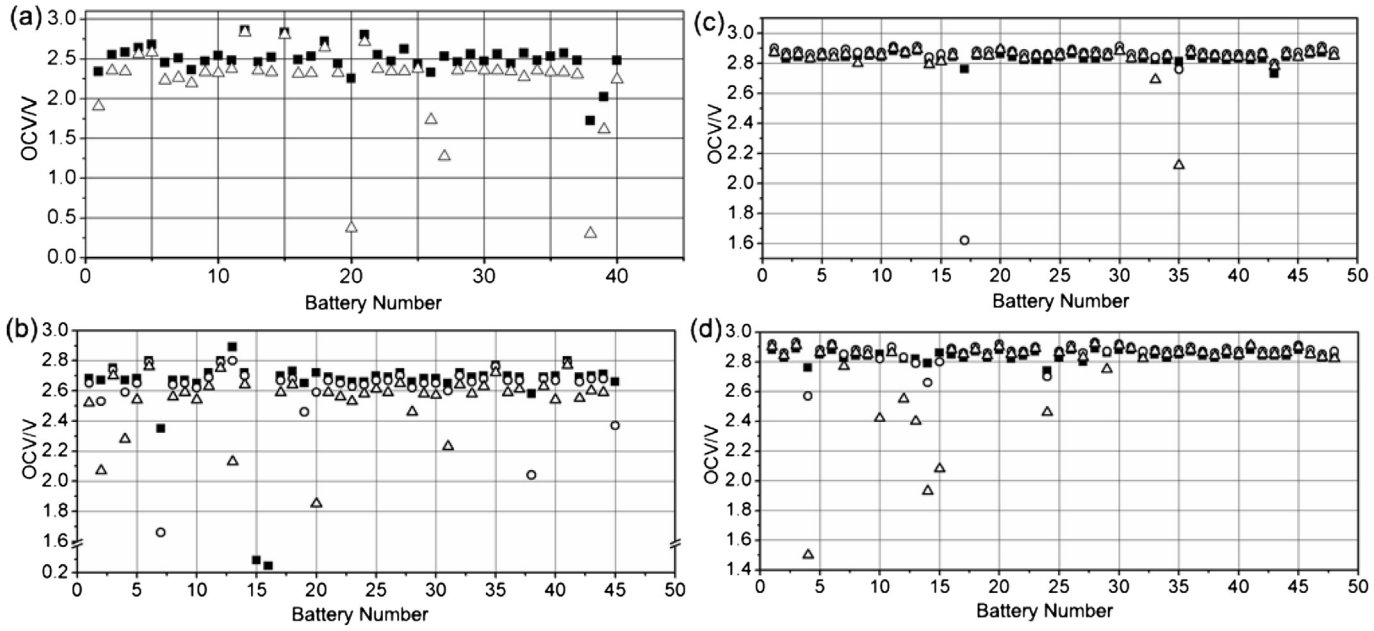

Fig. 2. The OCV varieties in self-discharge experiments for (a) LIPB I, (b) LIPB II, (c) LIPB III, and (d) LIPB IV, respectively. "■" stands for the LIPBs' OCVs before self-discharge experiment, and "○" and "Δ" for the OCVs after one- and 4-day storage at 45 °C in self-discharge experiments, respectively.

shows a much lower self-discharge as compared with LIPB II. The increase in OCV during self-discharge test implies the Li^+ ion diffusion in the active materials (mainly in the $LiFePO_4$ particles due to their much lower conductivity than that of the graphite) dominates the evolution of OCV as compared to the influence by the SEI films. This also indicates the formed SEI films are quite stable. The low OCV LIPB III takes up only 4.2%, and the unstable batteries (with OCV varieties larger than 0.10 V before and after self-discharge test) are 6.3%. The average OCVs before and after one- and 4-day storage are calculated to be as high as 2.84, 2.87, 2.85 V, respectively, demonstrating the small changes in OCVs during the self-discharge test, indicating a low self-discharge rate for LIPB III. The high stability of LIPB III is mainly derived from the more stable SEI films available because the activation processes mainly affected the composition and structure of SEI films (we will prove the formation of the stable SEI films by other methods later).

For the LIPBs treated by the activation processes with only aging but without charge–discharge cycle (others are the same to the activation processes LIPB III used, as shown in Table 1) (such batteries are denoted as LIPB IV), the average OCVs of LIPB IV are also as high as 2.85, 2.87, and 2.86 V before and after one- and 4-day storage, respectively. Additionally, most of the OCVs are also increased after one-day storage (Fig. 2d). The above two points indicate that the aging is advantage for the stability of the battery. From the OCV point of view, the SEI films formed during aging are more stable than those formed in the course of charge–discharge cycle, which is likely derived from the aging capable of stabilizing the SEI films likely via forming the more stable species and/or polymerization [35] (we will further discuss this below).

However, the OCV distribution for LIPB IV is much worse than that for LIPB III (Fig. 2c and d). The low OCV LIPB IV takes up as large as 12.5%, and the batteries with OCV variety larger than 0.10 V account for 14.6%, suggesting the aging could damage the stability of the battery if it is not first treated by charge–discharge cycle. On the other hand, the OCVs of LIPB IV are much higher than those of LIPB II, implying the aging has a stronger effect on the stability of the battery than the charge–discharge cycle. Furthermore, the LIPB III treated by the activation processes with both charge–discharge cycle and aging exhibits the best stability. Therefore, we can conclude that the main function of charge–discharge cycle is to protect the active materials against damage by the electrolyte during aging via forming the SEI films covering completely the surfaces of the active materials [14], and the aging can stabilize the stability of the SEI films formed during charge–discharge cycle. If the previously formed SEI films do not fully cover the surfaces of the electrodes, aging at high temperatures will possibly aggravates the unstability of the SEI films [32], leading to a large self-discharge of the battery reflected by its low OCV. Therefore, activation processes can affect the stability of LIPB greatly via affecting the formation and evolution of SEI films.

We also concern the capacity property of the LIPBs with OCVs higher than 2.50 V after self-discharge experiment. The results (Table 2) show that LIPB III has less low capacity batteries (time of discharge at 1.00 C to 2.00 V less than 60 min) (2.1%) than LIPB IV (16.7%). Correspondingly, LIPB III has more high capacity batteries (discharge time longer than 63 min) (55.3%) than LIPB IV (47.6%). Therefore, the batteries treated by the activation processes with both charge–discharge cycle and aging display a better stability, which is mainly due to the stable SEI films formed that could protect against the negative interactions between the active materials and the electrolyte. That is to say, aging could cause irreversible reactions between the active materials and the electrolyte if the formed SEI films could not completely cover the surfaces of the active materials previously. This also indicates charge–discharge cycle can yield the preliminarily stable SEI films that completely cover the active materials' surfaces, and the aging can consolidate the stability of the formed SEI films.

Table 2
Average resistances and capacity distributions of LIPBs treated by different activation processes.

No.	[a]r/mΩ	[b]Capacity distributions/%	
		<60 min	>63 min
LIPB II	11.78	3.0	66.7
LIPB III′	12.79	\	\
LIPB III	12.85	2.1	55.3
LIPB IV′	12.05	\	\
LIPB IV	12.15	16.7	47.6

[a] Average resistances after activation processes.
[b] Discharge at 1.00 C to 2.00 V with the discharge time limited to 90 min only for the batteries with OCVs higher than 2.50 V. The capacity is counted as the discharge time.

LIPB II shows a small percentage of the low capacity batteries (3.0%) and a relatively high proportion of the high capacity batteries (66.7%) though its low OCV (Table 2), which is mainly resulted from the formed SEI films not consuming many lithium species as will be discussed in the following concerning internal resistance.

Analyzing the evolution of internal resistance of LIPB can shed new light on the evolution of the formed SEI films. The method for determining the internal resistance is based on the alternating current perturbation mode (other literature also used the similar method to determine the electrical conductivity of an electrode [36]). The variety in internal resistance is mainly related to the evolution of the SEI films, since Li^+ diffusion resistance in electrolyte, charge transfer resistance, and Ohm contact resistance are basically the same for each LIPB due to the same in the battery materials used and in the battery assembly technologies adopted. On the basis of these considerations, we record the internal resistances of LIPBs previously treated by the activation processes either with or without charge–discharge cycle but both with 2-day aging (the corresponding batteries are denoted as LIPB III′ and LIPB IV′, respectively), and also record those of LIPB III and LIPB IV together to investigate the effect of aging on the evolution of internal resistance. The results (Table 2) show that the internal resistances increase with aging duration (increasing from 12.79 mΩ for LIPB III′ to 12.85 mΩ for LIPB III and from 12.05 mΩ for LIPB IV′ to 12.15 mΩ for LIPB IV), implying the SEI films grow with aging. However, it is discernable that the batteries treated by the activation with charge–discharge cycle have larger internal resistances compared to those without charge–discharge cycle under the same aging duration in the activation processes (i.e. 12.79 mΩ for LIPB III′ vs 12.05 mΩ for LIPB IV′ and 12.85 mΩ for LIPB III vs 12.15 mΩ for LIPB IV) (Table 2). This indicates that the charge–discharge cycle contributes to the formation of SEI films. Furthermore, the internal resistance varieties during aging is smaller for the batteries treated by the activation with charge–discharge cycle (only 0.06 mΩ variety between LIPB III′ and LIPB III, Table 2) than those without the cycle (0.10 mΩ range from LIPB IV′ to LIPB IV, Table 2), suggesting the SEI films of the LIPBs treated by the activation with charge–discharge cycle besides aging are more stable. We have known that the capacity property of LIPB III is better than that of LIPB IV. So the relatively larger internal resistance of LIPB III is not merely derived from the formation of more lithium species, but more importantly, should be also from the stabilization of the formed SEI films in the course of aging. Such stabilization will be discussed a little later. On the other hand, the LIPB II treated by the activation with only charge–discharge cycle, with the much worse stability than LIPB III and LIPB IV, has the relatively lower average internal resistance (11.78 mΩ, Table 2), which also indicates the aging can induce the formation of SEI films and further stabilize them. Therefore, both

charge–discharge cycle and aging are indispensable for the stability of LIPB.

The relatively low internal resistance of LIPB II (11.78 mΩ, Table 2) indicates the formed SEI films did not consume many active lithium, which is mainly responsible for the high capacity demonstrated. However, this is a sacrifice to the low stability of the batteries.

Next we will further prove that the low OCV issue occurring on LIPB is mainly attributed to the unstable SEI films formed. We have known that charge–discharge cycle and aging are the important factors for the achievement of the stable LIPB. In the following, we use the above two factors to treat the low OCV LIPB I to check whether the batteries can be repaired or not.

The used repair technology is listed below:

(1) Constant current/voltage controlled charge at 0.50 C to 3.65 V with the cut-off current of 0.05 C and the charge time limited to 180 min, followed by 10-min relaxation;
(2) Constant current discharge at 1.00 C to 2.00 V with the discharge time limited to 90 min, followed by 10-min relaxation;
(3) Cycle of the above two steps for one time;
(4) Constant current/voltage controlled charge at 0.50 C to 3.65 V with the cut-off current of 0.05 C and the charge time limited to 180 min.
(5) Aging of the batteries at 45 °C for 7 days.

After repair of the batteries, we carried out the self-discharge experiment, and the results (Fig. 3) show that all OCVs are higher than 2.80 V, and the average OCV reaches 2.89(4) V after repair; after self-discharge experiment, most OCVs only change slightly, and the average OCV is still as high as 2.89(2) V excluding the two relatively low OCV batteries (i.e. number 20 and 38 batteries) (Fig. 3). The low-OCV batteries only take up 2.5%, and the proportion of the unstable batteries (with OCV variety larger than 0.10 V before and after self-discharge test) is merely 5%. These indicate that the repair technology is effective for repairing the low-OCV batteries. Such a technology can only change the surface states of electrodes, that is, the properties of the SEI films.

We also repaired the low-OCV LIPB III and LIPB IV by using the above repair technology, and the results showed that two of the low-OCV LIPB III could be repaired. However, for the low-OCV LIPB IV, the unstable batteries (with OCV variety larger than 0.10 V) still took up 57.1% in the repaired batteries. This indicates that it is difficult to repair the low-OCV LIPB previously treated by only aging in the activation processes. The main reason should be the high-temperature storage of the LIPB, without previous forming the surface passivation layers on the electrodes by charge–discharge cycle, causing the destruction of the surface structures of the electrodes (further discussed below).

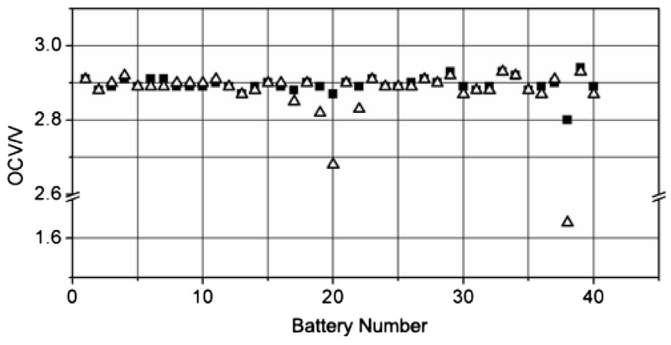

Fig. 3. OCV varieties in self-discharge test for LIPB I after repair. "■" and "Δ" stand for the OCVs before and after self-discharge test, respectively.

The low OCV issue is resulted from the unstable SEI films causing self-discharge in LIPB as discussed above. The self-discharge phenomenon also can be found by determining the capacity retention of the battery.

We studied the capacity retention of two LIPBs, a low-OCV LIPB (with original OCV of 1.51 V) and a normal-OCV one (with original OCV of 2.79 V). The above two LIPBs were first charged (at 0.50 C to 3.65 V with the cut-off current of 0.05 C and the charge time limited to 180 min) to full charged states, and then stored at room temperature for 15 days, followed by determining their remaining capacities (by discharging the batteries at 1.00 C to 2.00 V). The results (Table 3) show that the original and remaining capacities of the low- and normal-OCV LIPBs are 1160.1, 1096 and 1191.3, 1138.3 mAh, respectively. So the capacity retentions are calculated to be 94.5% and 95.6%, respectively, demonstrating the relatively poor capacity retention for the low-OCV LIPB. Thus, the low-OCV LIPB displays relatively large self-discharge. We also can understand this from the viewpoint of internal resistance variety. The internal resistance of the low-OCV LIPB is increased from 13.8 to 14.7 mΩ after storage (Table 3). However, the internal resistance of the normal-OCV LIPB does not change obviously during storage (the internal resistance keeps at 13.3 mΩ, Table 3). The increase in the internal resistance of the low-OCV LIPB indicates the development of the SEI films, which can consume the new Li^+ ions coming from the self-discharge of the battery. In addition, the unstable SEI films can improve the side reactions between the active materials and the electrolyte, also leading to capacity loss. Therefore, low OCV can cause capacity loss.

We also analyze the morphology natures of the electrodes of LIPBs with different activation treatments. Before activation, both the cathode $LiFePO_4$ particles (with relatively larger sizes compared to those of the carbon black) and the anode graphite particles are smooth in the surfaces and the boundaries are distinct (Fig. 4a and b). After activation, the whole surfaces of the electrodes of LIPB III with normal OCV turn out to be relatively smooth, and the previous distinct boundaries of the particles become relatively vague (Fig. 4c and d), which indicate the formation of SEI films on the surfaces of the two electrodes. However, for a low-OCV LIPB IV, the surfaces of both cathode and anode change to coarse (Fig. 4e and f), which is mainly due to the unstable SEI films causing the deterioration of the surface structures of the active materials by the electrolyte especially at high temperatures. The poor surface structures inversely lead to the difficult formation of the stable SEI films (as discussed above on the repair of the low-OCV LIPB IV). Such unstable SEI films can cause large self-discharge reflecting by the low OCV and the capacity loss of the battery. The capacity loss also can cause the irreversible transformation between $FePO_4$ and $LiFePO_4$, and resulting in coarsening of the particles [37].

For further proving the formation of SEI films, we analyzed the surface components of the electrodes of LIPBs with different OCVs

Table 3
Changes in capacities and internal resistance of LIPBs with different OCVs during storage.

	OCV/V	Capacity change/mAh		Capacity retention/%	Internal resistance change/mΩ	
		Before storage	After 15-day storage		Before storage	After 15-day storage
Low-OCV LIPB	1.51	1160.1	1096	94.5	13.8	14.7
Normal-OCV LIPB	2.79	1191.3	1138.3	95.6	13.3	13.3

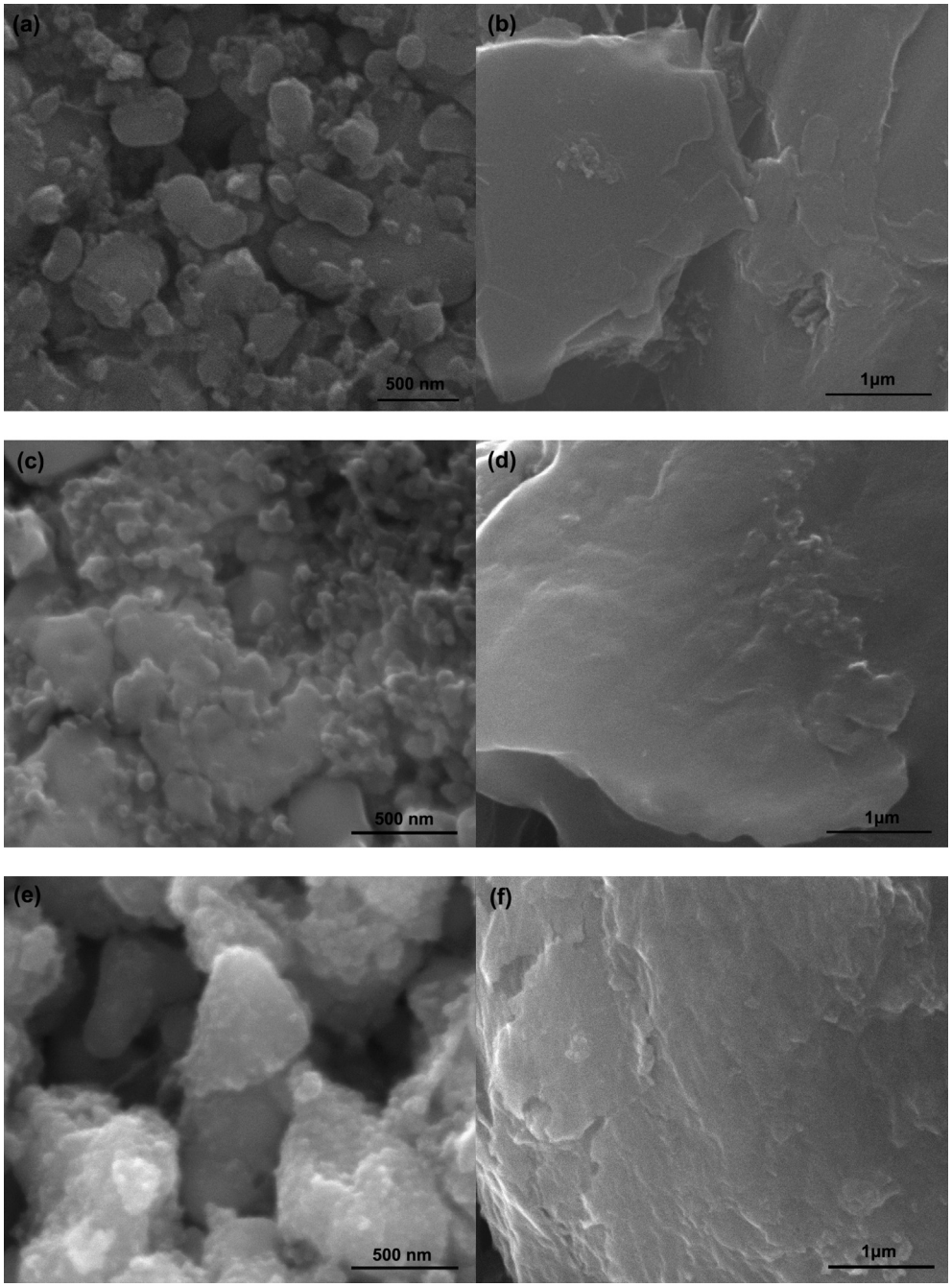

Fig. 4. SEM images of (a, c, e) cathodes and (b, d, f) anodes for (a, b) pristine electrodes without assembly to a battery, (c, d) the normal-OCV LIPB III, and (e, f) the low-OCV LIPB IV, respectively.

by EDS, and the results are shown in Table 4. For the cathode of the high-OCV battery (previously suffered from self-discharge test), it is clearly observed that the atomic ratio of C is increased, and the atomic ratios of O, Mg, P, and Fe are all decreased as compared to the pristine cathode, which indicates that the surface films mainly composed of carbon-containing species were formed on the cathode. Similar phenomena occur on the cathode of the low-OCV battery (previously suffered from self-discharge test). However, the increased degree of the content of C and the decreased degrees of the contents of O, P, and Fe are both smaller than those of the high-OCV battery, and the cathode distinctly contains Mg. The above two points reveal that the formed surface films on the cathode of the low-OCV battery are relatively thin and/or imperfect.

For both the anodes of the high- and the low-OCV batteries, the C content is decreased and the O and F contents are increased, which means the formation of SEI films. However, the relatively lower C content and the higher O content for the anode of the high-OCV battery as compared to the low-OCV one indicates that more oxygen-containing carbon species were generated in the formed SEI films for the former. Such SEI films composed of more oxygen-containing carbon species are more stable.

Therefore, both cathode and anode of LIPB were formed SEI films, and the films formed on the electrodes of the high-OCV LIPB are more stable than those of the low-OCV one.

We also used FTIR to study the differences in the surface states of the electrodes of the LIPBs with different OCVs, and the results

Table 4
Surface components of the pristine electrodes and the electrodes of the high-OCV and the low-OCV batteries obtained by EDS mapping.

		Atomic%				
		C	O	Mg	P	Fe
Cathodes	Pristine	31.69	49.14	0.33	10.24	8.60
	High-OCV	41.18	41.60	\	9.19	8.03
	Low-OCV	35.05	45.92	0.45	10.17	8.42
		Atomic%				
		C	O	F	[a]Cu	
Anodes	Pristine	96.02	2.96	1.02	0.00	
	High-OCV	90.54	4.81	4.18	0.47	
	Low-OCV	90.70	3.33	5.76	0.22	

[a] The Cu component comes from the Cu substrate.

are shown in Fig. 5. For the pristine cathode (Fig. 5a, black curve), the peaks at 1126, 1089, 1009, 661, 592, 563, and 488 cm^{-1} are derived from $LiFePO_4$ [38], the peaks above 1166, 889, and 848 cm^{-1} are attributed to PVDF [39,40], and the peaks centered at 530 and 413 cm^{-1} can be assigned to MgO. The cathode of the low-OCV battery (without aging treatment) presents the similar IR spectrum (Fig. 5a, red curve) to that of the pristine cathode, indicating the low-OCV battery's cathode did not effectively form SEI films. However, for the IR spectrum of the cathode of the high-OCV battery (selected from LIPB III) (Fig. 5a, blue curve), two new peaks appear at 508 and 437 cm^{-1}, and two broad bands at 1530 and 1430 cm^{-1} are discernible, suggesting Li_2CO_3 was formed on the surfaces of the cathode [41]. Li_2CO_3 is considered to be an important compound for the reversibility and high-temperature stability of the LIPB [20,42]. In addition, the occurrence of the broad bands above 3800, 1700, 1530, and 1430 cm^{-1} with many weak peaks implies the formation of carboxylates and carbonate species (such as Li_2CO_3) on the cathode with different adsorption states [43–45]. Moreover, two new peaks of PVDF occur at 1213 and 1253 cm^{-1}, and the previous $LiFePO_4$ peak at 661 cm^{-1} is divided into two peaks (at 695 and 668 cm^{-1}), which mean that the surface states of the cathode have been modified. The above three points together suggest that the surfaces of the cathode of the high-OCV battery formed SEI films mainly composed of carbon-containing species such as carboxylates and carbonate species (like Li_2CO_3) evidently.

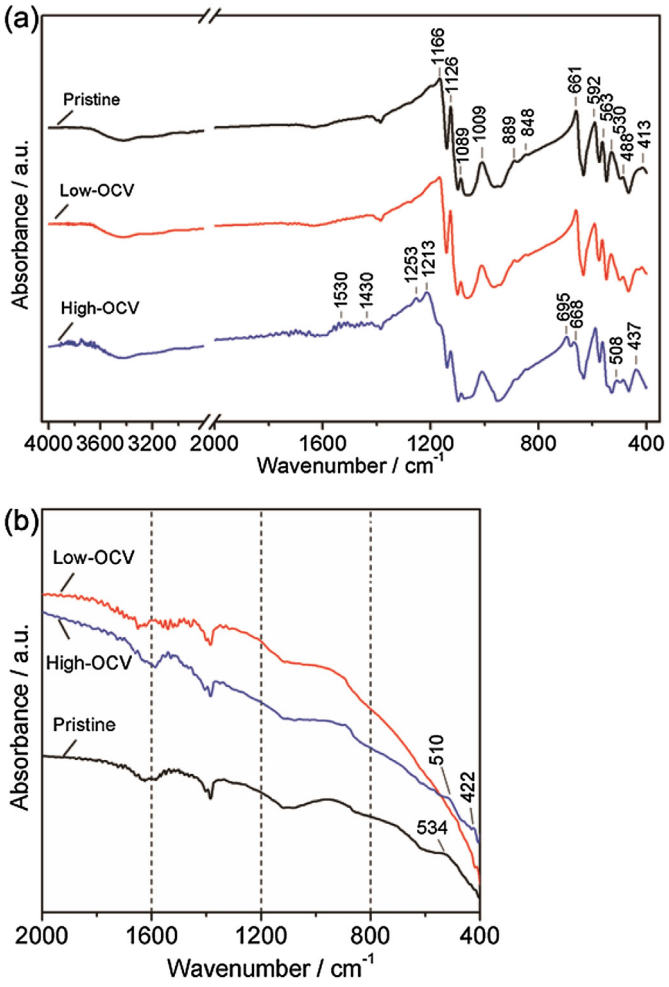

Fig. 5. FTIR spectra of (a) the cathodes and (b) the anodes of LIPBs, respectively. Black curves: the pristine electrodes (without wetted by electrolyte); red curves: the electrodes of the low-OCV battery; blue curves: the electrodes of the high-OCV battery. No obvious peak occurs in the range between 2000 and 2800 cm^{-1} for the spectra in panel a. (For interpretation of the references to color in this figure legend, the reader is referred to the web version of this article.)

The IR spectra of different anodes are shown in Fig. 5b. The IR spectrum of the pristine anode (Fig. 5b, black curve) mainly shows three broad bands, 1600–1400, 1400–1100, 1100–850 cm^{-1}, respectively. These bands are mainly derived from carboxylates and carbonate species [43–46] mainly resulted from the oxidation treatment to the graphite for improving its stability. The broad band above 1600–1400 cm^{-1} primarily reflects the characteristic of the carbonate groups, and the broad band above 1400–1100 cm^{-1} contains more features of the carboxylate components. In addition, a weak broad band at 534 cm^{-1} occurring on the pristine anode is assignable to the vibration of LiF (which was doped in the structure of the graphite for enhancing the charge–discharge reversibility).

For the IR spectrum of the anode of the low-OCV battery (Fig. 5b, red curve), the broad band above 1600–1400 cm^{-1} becomes weak, while the broad band ranging from 1400 to 1100 cm^{-1} turns to relatively stronger, as compared to that of the pristine anode. Thus, the anode surfaces adsorb more carboxylates whose stability is weaker than carbonates. Additionally, the previous IR peak of LiF at 534 cm^{-1} disappears, implying that the surfaces of the anode were covered by SEI films.

Just opposite to the case of the low-OCV battery, the IR spectrum of the high-OCV battery anode (Fig. 5b, blue curve) shows a stronger broad band above 1600–1400 cm^{-1} as compared to that above 1400–1100 cm^{-1}, indicating the anode was adsorbed by more carbonates (contributing to the higher stability of the SEI films) than carboxylates. Furthermore, two weak peaks at 510 and 422 cm^{-1} appear, suggesting Li_2CO_3 was indeed formed on the anode surfaces, which also contributes to the stability of the SEI films.

On the basis of the above discussion, SEI films were formed on the anode's surfaces after the battery was treated by activation processes. The SEI films formed on the surfaces of the high-OCV battery's anode were stable. However, the anode covered by the unstable SEI films can cause the relatively large self-discharge as indicated by a low OCV of the battery.

Mild oxidation of graphite in the processes of material preparation forms a variety of surface groups containing carboxylic groups, C=O double bonds, and anhydride-types groups. So Li alkoxy and Li carboxylate groups can be facilely formed in the activation processes and gas generation is also reduced, making the anode stay stability even when the battery is stored at high temperatures. During aging, the more stable Li_2CO_3 [20,42] was also formed on the surfaces of the anode. The formed Li_2CO_3 should be mainly derived from the decomposing of the surface adsorbed carboxylates and/or alkyl carbonates in the course of aging [47]. The

intensity evolutions of the two broad IR bands above 1600–1400 cm^{-1} and 1400–1100 cm^{-1} from the IR spectrum of the low-OCV battery's anode to that of the high-OCV battery's anode (Fig. 5b) also confirm this point. In this way, a strongly adherent surface layer was formed on the anode's surfaces, resulting in a good electrode passivation, thus reducing its irreversible capacity and increasing its stability upon storage even at high temperatures.

For cathode, the carbon coating and MgO modification protect the $LiFePO_4$ particles from corrosion by the acid in electrolyte. The carbon coating also can promote the formation of the surface passivation films, providing the $LiFePO_4$ particles with a stronger protect against the irreversible reactions with the electrolyte [48]. In this case, aging the $LiFePO_4$ cathode can avoid the capacity fading arising from the side reactions between $LiFePO_4$ particles and electrolyte. What's more, Li_2CO_3 was generated on the cathode's surfaces during aging, as discussed in Fig. 5a. Li_2CO_3 also can partially neutralize the trace HF in solution phase. Such SEI films containing Li_2CO_3 are more stable and can inhibit the side reactions between $LiFePO_4$ and electrolyte, contributing to the high stability of the cathode.

Therefore, the LIPB with low self-discharge rate, high capacity, and stable internal resistance is mainly resulted from the formation of the stable SEI films. Charge–discharge cycle and aging are the two critical factors for the formation of the stable SEI films from the angle of activation processes. Carbon coating and Mg^{2+} doping for $LiFePO_4$ particles and mild oxidation treatment to the graphite particles with smooth surfaces are both conductive to the formation of the stable SEI films. Charge–discharge cycle induces the generation of the surface passivation layers completely covering the electrodes' surfaces, and aging can enhance the stability of the passivation layers by decomposing the surface adsorbed organic species to more "inorganic" compounds (such as carboxylates) or even carbonates (such as Li_2CO_3) which demonstrate more stability and stronger adherent to the electrodes.

At last but not least, we compare the cycling properties of a high-OCV LIPB (selected from LIPB III) and a low-OCV LIPB (selected from LIPB IV) to elucidate the significance of the proper activation processes (i.e. the stability of the SEI films) on the stability of the battery. The results (Fig. 6) show that the high-OCV LIPB demonstrates excellent cycling reversibility. The capacity retention is still as high as 95% after 500 cycles at a charge/discharge rate of 5.00 C (red circle in the web version in Fig. 6). However, the low-OCV LIPB exhibits much worse cycling property, as can be seen that large capacity fading occurs even in 50 cycles (black quadrangle in Fig. 6) at a charge/discharge rate of 1.00 C. These results further indicate that the activation processes play an important role in the stability of a Li-ion battery.

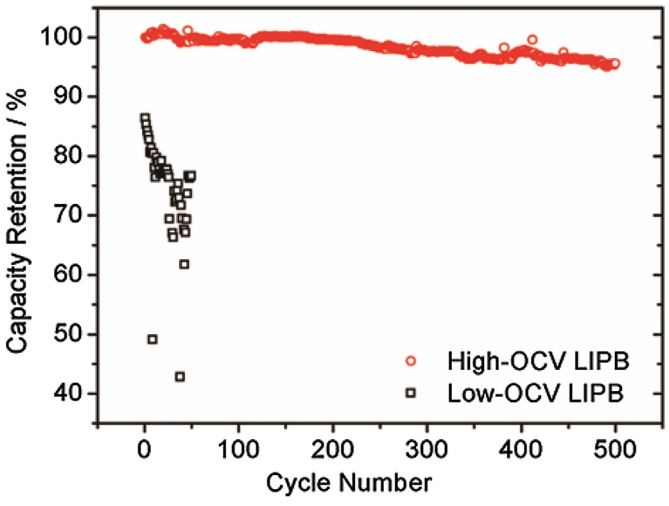

Fig. 6. Cycle curves of a high-OCV LIPB (selected from LIPB III) at 5.00 C and a low-OCV LIPB (selected from LIPB IV) at 1.00 C, respectively.

4. Conclusions

Activation processes can affect greatly the stability of LIPB by influencing the properties of SEI films. Charge–discharge cycle and aging are the two important factors for obtaining stable SEI films. The good stability of LIPB can be reflected by its high OCV, a small OCV variety, a stable internal resistance, and a good capacity. The low OCV LIPBs can be repaired by using the treatments similar to the activation processes with charge–discharge cycle and aging, indicating the stability of the LIPB can be affected to a large extent by the properties of the formed surface films. The formation of SEI films were confirmed by SEM, EDS, and FTIR spectra. The electrodes of the stable LIPB had the smooth surface layers containing the more stable carboxylate and carbonate species generated during aging. Charge–discharge cycle mainly contributed to the formation of the surface passivation films completely covering the electrodes' surfaces, and aging could stabilize such surface films by inducing the generation of the more stable carboxylates or even carbonates such as Li_2CO_3. The LIPBs treated by the proper activation processes demonstrated high stability and excellent uniformity, which is beneficial for various practical applications, especially for electric vehicles and other large battery system.

Acknowledgments

This work was supported by the National Nature Science Foundations of China (Grant 21273290, 20973205 and 91323101), the Natural Science Foundations of Guangdong Province (Grant 8151027501000095 and S2013030013474), and the Program of Cooperation of Industry, Education and Academy of Guangdong Province (2011B090400618 and 2011A090200036).

References

[1] S.S. Zhang, J. Power Sources 162 (2006) 1379–1394.
[2] J.S. Gnanaraj, E. Zinigrad, M.D. Levi, D. Aurbach, M. Schmidt, J. Power Sources 119–121 (2003) 799–804.
[3] H.F. Xiang, H. Wang, C.H. Chen, X.W. Ge, S. Guo, J.H. Sun, W.Q. Hu, J. Power Sources 191 (2009) 575–581.
[4] N. Dupré, J.-F. Martin, J. Degryse, V. Fernandez, P. Soudan, D. Guyomard, J. Power Sources 195 (2010) 7415–7425.
[5] D. Aurbach, Y. Talyosef, B. Markovsky, E. Markevich, E. Zinigrad, L. Asraf, J.S. Gnanaraj, H.-J. Kim, Electrochim. Acta 50 (2004) 247–254.
[6] J.S. Gnanaraj, E. Zinigrad, L. Asraf, M. Sprecher, H.E. Gottlieb, W. Geissler, M. Schmidt, D. Aurbach, Electrochem. Commun. 5 (2003) 946–951.
[7] C.M. Doherty, R.A. Caruso, C.J. Drummond, Energy Environ. Sci. 3 (2010) 813–823.
[8] M. Wagemaker, F.M. Mulder, A.V. Ven, Adv. Mater. 21 (2009) 2703–2709.
[9] P. Gibot, M. Casas-Cabanas, L. Laffont, S. Levasseur, P. Carlach, S. Hamelet, J.-M. Tarascon, C. Masquelier, Nat. Mater. 7 (2008) 741–747.
[10] B. Kang, G. Ceder, Nature 458 (2009) 190–193.
[11] R. Dominko, M. Bele, M. Gaberscek, M. Remskar, D. Hanzel, S. Pejovnik, J. Jamnik, J. Electrochem. Soc. 152 (2005) A607–A610.
[12] H.C. Shin, W.I. Cho, H. Jang, Electrochim. Acta 52 (2006) 1472–1476.
[13] G.T.K. Fey, T.L. Lu, J. Power Sources 178 (2008) 807–814.
[14] C.M. Doherty, R.A. Caruso, B.M. Smarsly, C.J. Drummond, Chem. Mater. 21 (2009) 2895–2903.
[15] N.N. Sinha, C. Shivakumara, N. Munichandraiah, ACS Appl. Mater. Interfaces 2 (2010) 2031–2038.
[16] D. Choi, P.N. Kumta, J. Power Sources 163 (2007) 1064–1069.
[17] C. Delacourt, P. Poizot, S. Levasseur, C. Masquelier, Electrochem. Solid-State Lett. 9 (2006) A352–A355.
[18] M. Wissler, J. Power Sources 156 (2006) 142–150.
[19] L. Wang, F. Zhou, Y.S. Meng, G. Ceder, Phys. Rev. B 76 (2007) 165435.
[20] K. Tasaki, S.J. Harris, J. Phys. Chem. C 114 (2010) 8076–8083.
[21] R.P. Ramasamy, J.W. Lee, B.N. Popov, J. Power Sources 166 (2007) 266–272.

[22] A. Augustsson, M. Herstedt, J.-H. Guo, K. Edstrom, G.V. Zhuang, P.N.J. Ross, J.-E. Rubensson, J. Nordgren, Phys. Chem. Chem. Phys. 6 (2004) 4185–4189.
[23] S. Leroy, F. Blanchard, R. Dedryvere, H. Martinez, B. Carre, D. Lemordant, D. Gonbeau, Electrochim. Acta 53 (2008) 3539–3546.
[24] J. Vetter, P. Novák, M.R. Wagner, C. Veit, K.C. Moller, J.O. esenhard, M. Winter, M. Wohlfahrt-Mehrens, C. Vogler, A. Hmmouche, J. Power Sources 147 (2005) 269–281.
[25] A.M. Andersson, K. Edsröm, J. Electrochem. Soc. 148 (2001) A1100–A1109.
[26] K. Xu, S. Zhang, T.R. Jow, Electrochem. Solid-State Lett. 6 (2003) A117–A120.
[27] Y. Sundarayya, S.K.C. Kumara, C.S. Sunandana, Mater. Res. Bull. 42 (2007) 1942–1948.
[28] D. Aurbach, M.D. Levi, E. Levi, H. Teller, B. Markovsky, G. Salitra, U. Heider, L. Heider, J. Electrochem. Soc. 145 (1998) 3024–3034.
[29] Y. Matsuo, R. Kostecki, F. McLarnon, J. Electrochem. Soc. 148 (2001) A687–A692.
[30] D. Aurbach, B. Markovsky, G. Salitra, E. Markevich, Y. Talyossef, M. Koltypin, L. Nazar, B. Ellis, D. Kovacheva, J. Power Sources 165 (2007) 491–499.
[31] M. Kerlau, R. Kostecki, J. Electrochem. Soc. 153 (2006) A1644–A1648.
[32] K. Amine, J. Liu, I. Belharouak, Electrochem. Commun. 7 (2006) 669–673.
[33] N. Meethong, Y.-H. Kao, S.A. Speakman, Y.-M. Chiang, Adv. Funct. Mater. 19 (2009) 1060–1070.
[34] T. Nakajima, J. Fluorine Chem. 128 (2007) 277–284.
[35] Y.-S. Hu, R. Demir-Cakan, M.-M. Titirici, J.-O. Mller, R. Schigl, M. Antonietti, J. Maier, Angew. Chem. Int. Ed. 47 (2008) 1645–1649.
[36] J.-H. Lee, H.-H. Kim, G.-S. Kim, D.-S. Zang, Y.-M. Choi, H. Kim, D.K. Yi, W.M. Sigmund, U. Paik, J. Phys. Chem. C 114 (2010) 4466–4472.
[37] S.C. Nagpure, S.S. Babu, B. Bhushan, A. Kumar, R. Mishra, W. Windl, L. Kovarik, M. Mills, Acta Mater. 59 (2011) 6917–6926.
[38] J.-K. Kim, G. Cheruvally, J.-H. Ahn, H.-J. Ahn, J. Phys. Chem. Solids 69 (2008) 1257–1260.
[39] G.J. Ross, J.F. Watts, M.P. Hill, P. Morrissey, Polymer 41 (2000) 1685–1696.
[40] Y. Peng, P. Wu, Polymer 45 (2004) 5295–5299.
[41] P. Pasierb, S. Komornicki, M. Rokita, M. Rekas, J. Mol. Struct. 596 (2001) 151–156.
[42] J.S. Shin, C.H. Han, U.H. Jung, S.I. Lee, H.J. Kim, K. Kim, J. Power Sources 109 (2002) 47–52.
[43] M. Lepage, T. Visser, F. Soulimani, A.M. Beale, A. Iglesias-Juez, A.M.J. Van der Eerden, B.M. Weckhuysen, J. Phys. Chem. C 112 (2008) 9394–9404.
[44] T. Shishido, T. Miyatake, K. Teramura, Y. Hitomi, H. Yamashita, T. Tanaka, J. Phys. Chem. C 113 (2009) 18713–18718.
[45] A. Yee, S.J. Morrison, H. Idriss, J. Catal. 191 (2000) 30–45.
[46] F.A. Andersen, L. Brečević, Acta Chem. Scand. 45 (1991) 1018–1024.
[47] G.V. Zhuang Jr., P.N. Ross, Electrochem. Solid-State Lett. 6 (2003) A136–A139.
[48] R. Dedryvère, M. Maccario, L. Croguennec, F. Le Cras, C. Delmas, D. Gonbeau, Chem. Mater. 20 (2008) 7164–7170.